SPRi signal amplification by organothiols-nanopattern

Patrícia Lisboa, Andrea Valsesia, Ilaria Mannelli, Pascal Colpo, François Rossi

European Commission JRC-IHCP ,
Nanotechnology and Molecular Imaging Unit, TP203, Via E. Fermi, 2749, 21027 Ispra (VA,) Italy
patrícia.lisboa@jrc.it

ABSTRACT

A 2D crystalline nanoarray of organothiols has been used for enhancing the detection sensitivity of Surface Plasmon Resonance assays. The nanoarrays have been fabricated by combining colloidal lithography and organothiol self assembly. In particular, immunoreaction produced by nano-spots with carboxylic function in a non-adhesive matrix of Polyethylene oxide (PEO) has been compared to uniform carboxylic surfaces. For the same concentration of analyte, the SPRi signal is much higher by using the 2D crystalline nanoarrayed surfaces.

Keywords: Nanoarray, Surface Plasmon Imaging, Immunosensor

1 INTRODUCTION

The implementation of sensor platforms providing high detection sensitivity is crucial for the design of new analytical devices [1]. Surface Plasmon Resonance (SPR) is a label free technique that is now well-established [2,3]. A constant effort is made for improving the detection sensitivity of plasmonic sensors for instance by using nanoparticles to increase the plasmonic effect in the Localized- SPR (L-SPR) technique [4,5]. Other advantages can be obtained by nanostructuring metallic thin films substrate, because the coupling of the light with Surface Plasmon Polariton SPP modes induces an electric field enhancement [6,7]. Moreover, sensor platforms designed with nanopatterned bio-adhesive/non-adhesive regions have shown increased sensing performance [8-12]. This report presents the study of the contribution of 2D-crystalline organothiol nanoarrays to the SPR imaging (SPRi) sensitivity. Organothiol nanoarray consists in bio-adhesive carboxylic nano-spots distributed in a non-adhesive background of Polyethylene oxide, a type of surface that has already shown a good potential for improved immobilization efficiency of proteins on surfaces [13]. The present study is based on the comparison of the detection of the immunoreaction obtained with nanoarrayed and uniform carboxylic surface by using Human IgG and anti-Human IgG.

2 RESULTS AND DISCUSSION

2.1 Nano-array fabrication and characterization

The gold surface of the SPRi chip was divided in two adjacent areas, one patterned with the nanoarray of two different organothiols (thiolated Polyethylene oxide (PEO) and mercaptohexadecanoic acid (MHD)) and the other uniformly functionalized by MHD.

To produce the nanoarray, three main steps are used. First, the gold coated prism is modified with MHD,. Next, a MHD/Gold nano-pattern is produced by plasma colloidal lithography and gold is finally functionalised with PEO to create a MHD/PEO nano-pattern [13].

The different steps of fabrication were characterized by Cyclic Voltammetry (results not shown). The redox reaction of the couple Fe(CN)63-/ Fe(CN)64- was monitored using the modified surfaces as working electrode with the conditions already explained in our past work [13]. For the bare gold electrode, the voltammogram presents the typical peak shape expected from a flat metallic surface. The functionalisation with MHD creates an insulating layer in the gold electrode reducing dramatically the collected current (no peaks present), thus indicating a good surface coverage. After the polystyrene beads deposition, etching and removal, the voltammogram presents a peak shape with lower definition compared to the bare gold one due to the presence of the MHD nano-areas. Finally after the PEO chemisorption, the surface is again well covered and presents a non-peak shape voltammogram.

Since the RMS roughness of the gold substrate and the RMS roughness of the nano-patterned surface are very close (<1 nm for both the surfaces), the Atomic Force Microscopy (AFM) analysis of the nano-arrayed surface presents a poorly distinguishable pattern from the topography image. Nevertheless, the 2-D Fast Fourier Transform (FFT) of the height function (Figure 1A, inset) clearly shows the presence of a hexagonal array corresponding to the pattern. The nano-pattern is well detected in the phase contrast image (Figure 1B) due to the different chemical properties of the two head group present on the surface. The surface is characterized by a 2D hexagonal lattice of carboxylic spots (9.8% of the total surface area) surrounded by PEO [13].

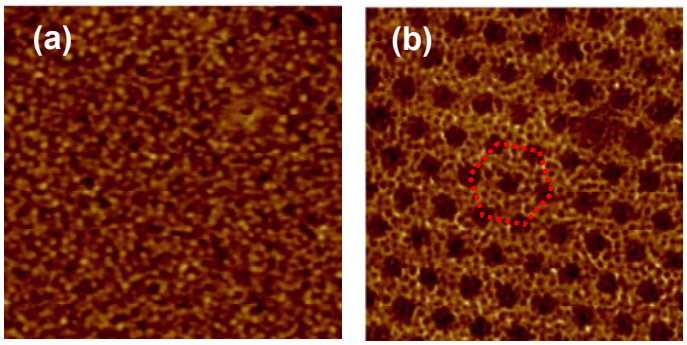

Figure 1-AFM characterization of the Nanoarray: A- topography image (vertical scale 0-5 nm); B- phase image (colour scale: -1° to 5°), the hexagonal arrangement of the COOH spots is highlighted by the dashed red line

2.2 SPRi measurements

The detection principle of the SPRi instrument is based on changes in the reflective index at the interface between gold and dielectric substrate due to the presence of immobilized biomolecules on the gold surface. These changes induce reflectivity variations that are monitored at a fixed angle by a 12 bit CCD camera as a gray level contrast [14].
The momentum matching of the incident light with the Surface Plasmon Polariton (k_{SPP}) at the interface between gold and the dielectric overlayer is ensured by the Kretschmann configuration. The condition for SPP matching with light is expressed by the formula [6,15]:

$$k_{SPP} = \frac{2\pi}{\lambda_0}\left(\frac{\varepsilon_{Au}\varepsilon_d}{\varepsilon_{Au}+\varepsilon_d}\right)^{1/2} = \frac{2\pi}{\lambda_0} n_p \sin(\vartheta) \qquad (1)$$

where λ_0 is the wavelength of the incident light (fixed at 810 nm), ε_{Au} is the dielectric function of the gold, ε_d is the dielectric constant of the dielectric interfacing the gold surface, n_p is the refractive index of the coupling prism and θ is the incident angle of light. Changes in ε_d cause a shift of the SPP momentum, which is detected by the angular detection of reflected light at the surface.
The first step of the SPRi experiment was the immobilization of the recognition element (Human IgG) followed by a blocking step. Reflectivity curves of figure 2 show that the SPRi reflectivity relative change is higher for the nanoarrayed surfaces than for the uniform surface.
Before the recognition of the analyte (anti Human IgG), a control of the interaction specificity was performed using anti-Ovalbumin. For both surfaces, the signal produced by anti OVA adsorption was less than 10% of the recognition signal, indicating a good specificity. After these steps, the recognition of the analyte (anti-Human IgG (Ab specific)) has been performed.

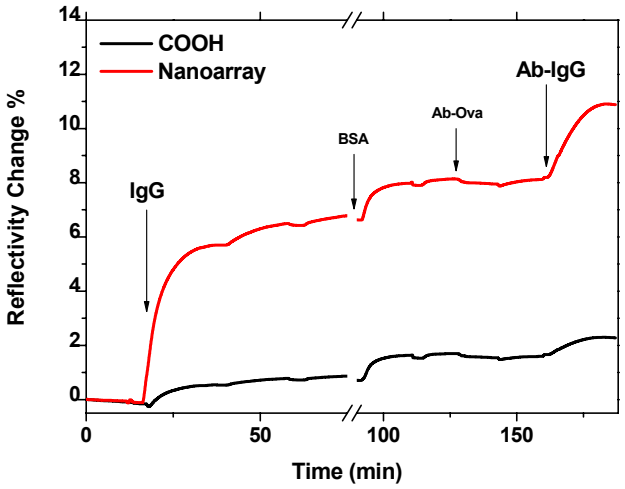

Figure 2-Kinetics of the SPRi immunoreaction experiments for the uniform and nanoarrayed COOH surface.

Since the active surface of the nanoarrayed MHD presents only 9.8% of the total area, one would expect the detection signal to be in the order of 10% of the signal obtained for the uniform MHD surface. On the contrary, the obtained reflectivity changes lead to an amplification of the signal by a factor 4 in the case of the nanopatterned surface. Such a discrepancy cannot not only be explained in terms of a higher efficiency of immobilization of the molecules by the nanopatterned surface, as already observed in other experiments performed with similar surfaces [10,11,16,17]. This abnormal increase of reflectivity is attributed to the 2-D crystalline arrangement of the nanopatterned surface, which leads to the interaction between the SPP modes and the regular spatial modulation of the dielectric constant of the surface above the gold film (2D photonic crystal (2D-PC)). Due to the very close refractive index of the two organothiols constituting the nanoarray (n_{MHD} = 1.45 and n_{PEO} = 1.42), as measured by ellipsometry), modulation has no effect before the exposure of the surface to the protein solution (i.e. the reflectivity curves of the uniformly functionalized COOH surface and the nanoarray are very similar (data not shown). But when IgG molecules adsorb on the nanospots, the surface forms a nanoarrayed substrate characterized by a higher contrast of the refractive index (n_{IgG} = 1.55 and n_{PBS} = 1.33); this nanoarray interacts with the SPP modes at the interface with gold. The interaction between the SPP and PC modes has been observed by many authors on different structured surfaces [7, 18, 19]. The coupling between SPP and PC is favored by the fact that the SPP wavelength is of the same order of magnitude of the lattice constant of the PC (being an hexagonal crystal, the PC has two lattice constant, a_1 = 500 nm and a_2 = 425nm). The SPP wavelength λ_{SPP} can be easily calculated from equation 1 as:

$$\frac{2\pi}{k_{SPP}} = \frac{\lambda_0}{n_p \sin\vartheta} \approx 651nm \qquad (2)$$

NSTI-Nanotech 2008, www.nsti.org, ISBN 978-1-4200-8505-1 Vol. 3

In other words, the matching conditions for the SPP momentum are now [19]:

$$k_{SPP} + i\frac{2\pi}{\vec{a}_1} + j\frac{2\pi}{\vec{a}_2} = \frac{2\pi}{\lambda_0} n_p \sin(\vartheta) \quad (3)$$

where $\vec{a}_1$ and $\vec{a}_2$ are the lattice vectors of the 2D-PC. The contributions of the 2D-PC to the momentum matching conditions are reflected in a change of reflectivity which is enhanced with respect to the one obtained on a non-structured surface. Since the SPRi system detects changes in the reflectivity at a fixed angle (where the derivative of the plasmonic resonance peak is maximum), this leads to an increment of the sensitivity of the SPRi detector.

The formation of the protein nanoarray which is, in the model previously described, responsible for the amplification of the SPRi signal has been confirmed by Atomic Force Microscopy (AFM) analysis. The AFM topographic image of the nanopatterned SPRi prism's surface after IgG-Ab-IgG recognition experiments, in dried conditions, is shown in Figure 3a. The selective immobilization of the proteins in the COOH arrayed nanospots is evidenced by the red circles in Figure 3a (a crystalline line is shown as an illustrative example). Also the profile along the blue line of a single nanospots confirms the formation of protein clusters selectively inside the COOH spots.

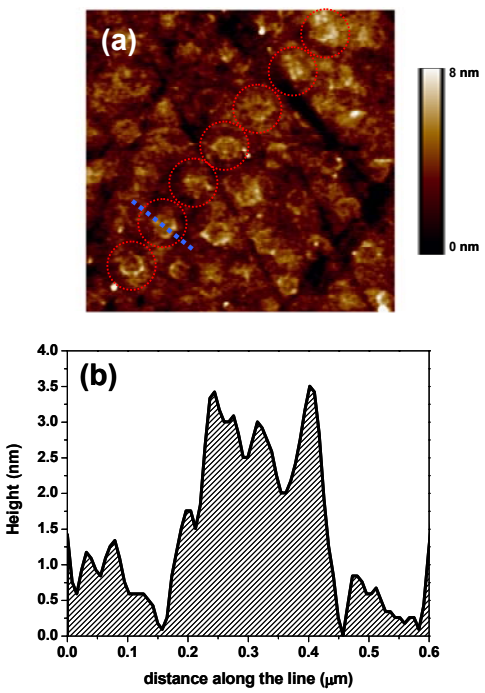

Figure 3- (a) 4 μm * 4 μm AFM scan of the nanopatterned SPRi prism's surface dried after protein absorption experiments. (b) Profile along the blue line in Figure 3a

In order to evaluate the performance of differently functionalized sensor surfaces, dose-response curves were measured with different analyte concentrations (Figure 4) by comparing the nanoarrayed surfaces with uniform COOH functionalized surfaces. In Figure 4 is also reported the Ab-Ova negative control for each concentration explored.

As a first approximation, the sensor response is linear for both the nanoarrayed and the COOH functionalized surfaces. The sensitivity of detection, *S* (defined as the variation of signal produced by an increment in the concentration of the analyte), can be calculated as the derivative of the calibration curve. Calculated values are reported in the inset in Figure 4. The sensitivity of the nanoarray is enhanced by a factor 5 with respect to the COOH one. These results indicate that coupling a commercial SPRi system with nanoarrayed surfaces characterized by bioadhesive motives in a non-bioadhesive matrix amplifies not only the signal by a factor of 4 but improves the sensitivity of the detection of the instrument.

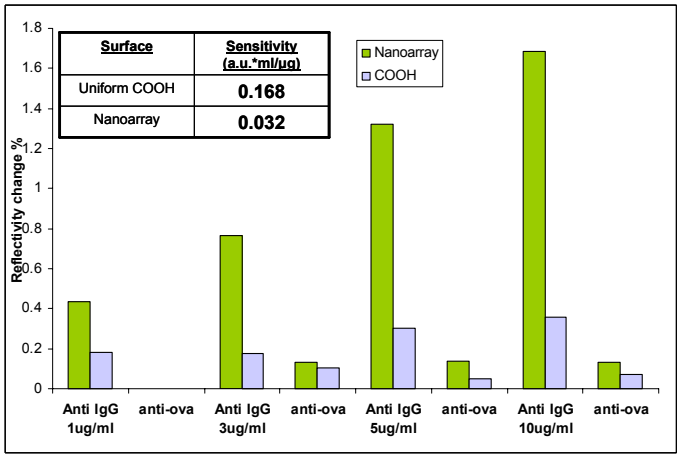

Figure 4-Calibration curves for the nanoarrayed and COOH functionalized surface and calculated sensitivity

3 CONCLUSIONS

This work demonstrates that the modification of the sensor surface with a 2D nano-crystalline pattern improves the SPRi detection. This improvement is due to the 2D crystalline arrangement of the surface that leads to the interaction between the SPP modes and the regular modulation of the dielectric constant of the surface above the gold film modifying the plasmon effect and consequently increasing the reflectivity. These results indicate that SPRi detection performance can be improved by the rational functionalisation of the prism surface with nanopatterns, characterized by spacing of the order of magnitude of the wavelength of the SPP wave. Moreover adhesive – nonadhesive nanopatterns are recognized to be good platforms for the correct immobilization of the biomolecules on biosensing surfaces.

REFERENCES

[1] Turner, A. P. F., Biosensors-Sense and Sensitivity. *Science* **290**, 1315-1317 (2000).

[2] Löfås, S. and Johnsson, B., *J. Chem. Soc., Chem. Commun* **21**, 1526-1528 (1990).

[3] Cooper, M. A., *Drug Discovery Today* **11**, 1061-1067 (2006).

[4] Haes, A. J., Zou, S., Schatz, G. C. and Duyne, R. P. V., *J. Phys. Chem. B* **108**, 109-116 (2004).

[5] Willets, K. A. and Duyne, R. P. V., *Annual Review of Physical Chemistry* **58**, 267-297 (2007).

[6] Barnes, W. L., Dereux, A., and Ebbesen T. W., *Nature* **424**, 824-830 (2003).

[7] Dintinger, J., Klein, S., Bustos, F., Barnes, W. L., and. Ebbesen, T. W, Strong, *Phys. Rev. B* **71**, 035424-1-5 (2005).

[8] Lee, K., Lee, K. B., Kim, E.Y., Mirkin, C. A., and Wolinsky S. M., *Nano-Letters **4*,** 1869-1872 (2004).

[9] Rosi, N. L. and C. A. Mirkin, *Chem. Rev.* **105**, 1547-1562 (2005).

[10] Valsesia, A., Colpo, P.,Meziani, T., Lisboa, P., Lejeune, M., Rossi, F., *Langmuir* **22**, 1763- 1767 (2006).

[11] Agheli, H., Malmstroem, J., Larsson, E. M., Textor, M., and Sutherland, D. S**.,** *Nano Letters* **6**, 1165-1171 (2006).

[12] Frederix, F., Bonroy K., Reekmans, G., Laureyn, W., Campitelli, A., Abramov, M. A., Dehaen, W. and Maes, G., *J. Biochem. Biophys. Methods* **58**, 67-74 **(**2004).

[13] Lisboa, P., Valsesia, A., Colpo, P., Gilliland, D., Ceccone, G., Papadopoulou-Bouraoui A., Rauscher, H., Reniero, F., Guillou, C. and Rossi, F., A*pplied Surface Science* **25**, 4796–4804 (2007).

[14] Guedon, P., Livache T., Martin, M., Lesbre, F., Roget,A., Bidan, G. and Levy, Y., *Anal.Chem.***72**, 6003-6009 (2000).

[15] Homola, J. , *Vol. 4* (Springer, Berlin -Heidelberg, 2006).

[16] Valsesia A., Mannelli, I.,. Colpo, P., Bretagnol, F., Ceccone, G. and Rossi, F., *NSTI Nanotechnology Conference and Trade Show - NSTI Nanotech 2007 Technical Proceedings*, *Vol. 4* ,586 – 589.

[17] Krishnamoorthy, S., Wright, J.P., Worsfold, O., Fujii, T. and Himmelhaus, M., *NSTI Nanotechnology Conference and Trade Show - NSTI Nanotech 2007 Technical Proceedings, Vol 4,* 590-593.

[18] Hibbins, A.P. and Sambles, J. R., *Appl. Phys.Lett*., **80**, 2410-2412 (2002).

[19] Wedge, S., Giannattasio, A. and Barnes, W.L*Organic Electronics* **8**, 136-147 (2007).